Determination of the effective conductivity of heterogeneous media by Brownian motion simulation

In Chan Kim
Department of Mechanical and Aerospace Engineering, North Carolina State University, Raleigh, North Carolina 27695-7910

S. Torquato[a)]
Department of Mechanical and Aerospace Engineering and Department of Chemical Engineering, North Carolina State University, Raleigh, North Carolina 27695-7910

(Received 16 April 1990; accepted for publication 21 June 1990)

A new Brownian motion simulation technique developed by Torquato and Kim [Appl. Phys. Lett. **55**, 1847 (1989)] is applied and further developed to compute "exactly" the effective conductivity σ_e of n-phase heterogeneous media having phase conductivities $\sigma_1, \sigma_2, ..., \sigma_n$ and volume fractions $\phi_1, \phi_2, ..., \phi_n$. The appropriate *first passage time* equations are derived for the first time to treat d-dimensional media ($d = 1$, 2, or 3) having arbitrary microgeometries. For purposes of illustration, the simulation procedure is employed to compute the transverse effective conductivity σ_e of a two-phase composite composed of a random distribution of infinitely long, oriented, hard cylinders of conductivity σ_2 in a matrix of conductivity σ_1 for virtually all volume fractions and for several values of the conductivity ratio $\alpha = \sigma_2/\sigma_1$, including perfectly conducting cylinders ($\alpha = \infty$). The method is shown to yield σ_e accurately with a comparatively fast execution time.

I. INTRODUCTION

The problem of determining the effective transport and mechanical properties of multiphase media (given the phase properties and volume fractions) has a long history, attracting the attention of such luminaries of science as Maxwell,[1] Rayleigh,[2] and Einstein.[3] Except for a few specially prepared artificial media, there are no exact analytical predictions of the effective properties of *random* multiphase systems for arbitrary phase properties and volume fractions, even for the simplest class of problems, i.e., properties associated with transport processes governed by a steady-state diffusion equation (e.g., conductivity, dielectric constant, diffusion coefficient, trapping rate, etc.).[4] For arbitrary phase properties and volume fractions, theoretical techniques basically fall into two categories: effective-medium approximations[5,6] and rigorous bounding techniques.[4,7-9] Relatively speaking, there is a paucity of work on "exact" simulations of the property of interest, especially for *continuum* models (e.g., distributions of particles in a matrix). Such "computer experiments" could provide unambiguous tests on the aforementioned theories for well-defined continuum models.

Most simulation studies of the past have attempted to solve the local governing differential equations for the fields (e.g., electric, temperature, concentration, etc.), subject to the appropriate boundary conditions at the multiphase interface of the computer-generated heterogeneous system, employing some numerical procedure such as finite differences or finite elements. This solution is obtained for each of a sufficiently large number of configurations and then the fields are configurationally averaged to get the effective properties. (For example, the effective electrical and thermal conductivities are defined by *averaged* Ohm's and Fourier's laws, respectively.) Unfortunately, this is a very wasteful way of obtaining the average behavior since there is a significant amount of information lost in going from the local to the average fields. It is not surprising, therefore, that such calculations become computationally exorbitant, even when performed on a supercomputer.

Accordingly, it is desired to employ a simulation technique which *directly* yields the desired average behavior, i.e., the effective property. Recently, Torquato and Kim[10] described a Brownian motion simulation technique to exactly yield effective properties of disordered heterogeneous media in which the transport process is governed by a steady-state diffusion equation:

$$D\nabla^2\Phi = -\gamma \text{ (in each phase)}. \tag{1}$$

Here Φ is some potential, D is the diffusion coefficient, and γ is a source term. Of course the appropriate boundary conditions at the multiphase interface must be satisfied. Thus, their algorithm can be applied to determine the effective electrical and thermal conductivity, dielectric constants, magnetic permeability, diffusion coefficient associated with flow past fixed obstacles, and the trapping rate associated with diffusion-controlled processes among static traps.

In order to illustrate their simulation technique, Torquato and Kim computed the diffusion-controlled trapping rate for perfectly absorbing, static spherical traps ($\Phi = 0$ at the trap surfaces). For this problem, one need only keep track of the mean square displacement of the Brownian particles until they get trapped, since this quantity (averaged over many walkers and realizations) is inversely proportional to the trapping rate. This is proved using a *first passage time analysis*. The essence of the method is to construct the

[a)] Author to whom all correspondence should be addressed.

 0021-8979/90/203892-12$03.00

largest possible concentric sphere of radius R about the Brownian particle (in the trap-free region) which does not overlap any trap particles, choose a point on the surface, record R^2, repeat the above steps until trapping is achieved, and finally compute the total mean square displacement $\langle \Sigma_i R_i^2 \rangle$ (which is proportional to the trapping rate). The method yielded the trapping rate highly accurately and was shown to have a very fast execution time. For example, the trapping rate at a fixed volume fraction for 490 spherical traps, 50 configurations, and 1000 random walkers per configuration has been computed on a VAX station 3100 in about 15 CPU minutes.

In this paper, we shall apply the general ideas of Torquato and Kim to develop a Brownian motion simulation technique to compute exactly the effective conductivity σ_e of an isotropic n-phase composite of arbitrary dimension d and microgeometry, given the phase conductivities $\sigma_1, \sigma_2, ..., \sigma_n$ and volume fractions $\phi_1, \phi_2, ..., \phi_n$. This class of problems is more complicated than the aforementioned trapping problem since it involves two new features: (1) different walking speeds in each phase and (2) a nonzero probability of reflection at the multiphase interface. In the many instances when the Brownian particle is far from the multiphase interface (i.e., when the particle walks entirely in one phase), one still constructs the largest concentric sphere of radius R about the particle which does not overlap any other phase material and chooses a point on the imaginary sphere surface randomly. The quantity R^2 is proportional to the mean first hitting time τ. The process is repeated, each time keeping track of R^2, until the walker comes within some very small distance of the multiphase interface. At this juncture, one computes the mean time associated with crossing the boundary τ_s and the probability of crossing the boundary, both of which are obtained here using first passage time theory. At some future time, the Brownian particle again will walk entirely in one phase and the above procedure is repeated. The effective conductivity σ_e is then related to the total mean square displacement or equivalently, the total mean time, in the limit of very large times.

We shall develop, for the first time, the appropriate first passage time equations for general d-dimensional composites ($d = 1, 2$, and 3) having arbitrary values of conductivity $\sigma_1, \sigma_2, ..., \sigma_n$. In order to illustrate the method, comprehensive computer simulation data for the effective conductivity σ_e are obtained for two-dimensional distributions of hard circular disks (i.e., infinitely long, oriented cylinders) of conductivity σ_2 in a matrix of conductivity σ_1. Conductivity data will be reported for virtually the entire volume fraction range and for $\alpha = \sigma_2/\sigma_1 = 10$, 50, and ∞. Using these results and a phase-interchange theorem, one can obtain corresponding results for the effective conductivity for $\alpha = 0.1$, 0.02, and 0, respectively. In a future paper, corresponding data will be obtained for distributions of hard spheres ($d = 3$).

This paper is organized as follows. In Sec. II, we define the effective conductivity σ_e in terms of certain averages of the Brownian motion trajectories and obtain the appropriate first passage time relations that apply in the immediate vicinity of the boundary between any two phases, say phase 1 and phase 2. The cases where $\sigma_2/\sigma_1 = 0$ and $\sigma_2/\sigma_1 = \infty$ are described separately. In Sec. III, we describe the simulation details to compute the effective conductivity for two-phase media composed of a distribution of infinitely long, oriented, hard cylinders of conductivity σ_2 in a matrix of conductivity σ_1 and report data for σ_e. In Sec IV, we make concluding remarks.

II. BROWNIAN MOTION FORMULATION

The basic relations employed by Torquato and Kim[10] to simulate the trapping rate were derived using a *first passage time analysis*. A similar analysis is to be formulated for the conductivity problem but here (as noted earlier) one must take into account two new features: (1) different walking speeds in each phase and (2) a nonzero probability of reflection at the interface. We first define the effective conductivity σ_e for isotropic n-phase composites with arbitrary values of $\sigma_1, \sigma_2, ..., \sigma_n$ in terms of certain averages of the Brownian motion trajectories. Next we derive, for the first time, the appropriate first passage time equations when a Brownian particle approaches an interface. We then examine the special case of one phase being perfectly insulating relative to a connected phase. Finally, we describe the instance of one phase that is infinitely conducting relative to a connected phase.

A. Effective conductivity

Consider a Brownian particle (conduction tracer) moving in an *homogeneous* region Ω of conductivity σ. Let the boundary be denoted by $\partial\Omega$ (see Fig. 1). If we define the mean hitting time $\bar{t}(\mathbf{x})$ as the mean time taken for the random walker initially at $\mathbf{x}$ to hit $\partial\Omega$ for the *first* time, it can be easily shown[11,12] that

$$\sigma\nabla^2\bar{t} = -1, \quad \text{in } \Omega$$
$$\bar{t}(\mathbf{x}) = 0, \quad \text{on } \partial\Omega. \tag{2}$$

If Ω is d-dimensional sphere of radius R and $\mathbf{x}$ is taken at the center of the sphere $\mathbf{x}_0$, the solution of (2) is

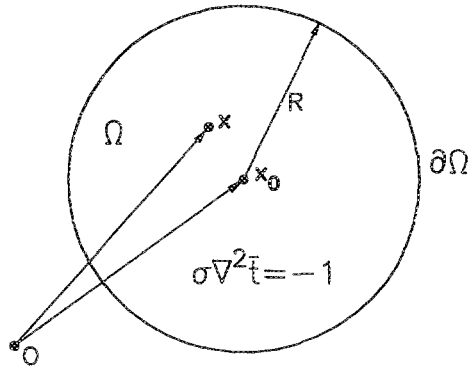

FIG. 1. Homogeneous medium of conductivity σ.

$$\tau(R) \equiv \bar{t}(\mathbf{x}_0; R) = R^2/2d\sigma. \tag{3}$$

Here $\tau(R)$ is defined to be the mean hitting time for a random walker initially at $\mathbf{x}_0$, the center of the sphere of radius R. Equation (3) can be rewritten as

$$\sigma = R^2/2d\tau(R). \tag{4}$$

Thus, if $\tau(R)$, which represents the first hitting time averaged over an infinitely large number of such Brownian trajectories, is known, then the conductivity σ can be obtained via Eq. (4). If an infinite medium is to be considered, the conductivity is given by

$$\sigma = R^2/2d\tau(R)|_{R\to\infty}. \tag{5}$$

The effective conductivity σ_e of an infinitely large composite medium can be computed in the same manner. Suppose we have a sphere of radius X which encompasses a general multiphase composite having conductivities $\sigma_1, \sigma_2, \ldots, \sigma_n$ (see Fig. 2). If we view this sphere as an effective homogeneous sphere of conductivity σ_e, we can write in the spirit of Eq. (4) that

$$\sigma_e = X^2/2d\tau_e(X). \tag{6}$$

Here $\tau_e(X)$ is the total mean time associated with the total mean square displacement X^2. Since every random walk path in the composite medium which first arrives at $\partial\Omega$ can be considered to be a sum of many smaller random walk path segments R_i's, each of which is a random walk path segment that lies entirely in a locally homogeneous medium of conductivity $\sigma^{(i)}$ (where $\sigma^{(i)}$ can be $\sigma_j, j = 1,2,\ldots,n$), Eq. (6) can be rewritten as

$$\sigma_e = \frac{X^2}{2d\langle \Sigma_i\, \tau(R_i)\rangle} = \frac{X^2}{2d\langle \Sigma_i\, R_i^2/2d\sigma^{(i)}\rangle}, \tag{7}$$

where angular brackets indicates an ensemble average.

In the actual simulation, in cases where the Brownian particle is far from the multiphase interface (which turns out to be a large portion of the time), we employ the same time-saving technique used by Torquato and Kim,[10] namely, one constructs the largest concentric d-dimensional sphere of radius R around the diffusing particle which just touches the multiphase interface. The Brownian particle then jumps in one step to a random point on the surface of this concentric sphere and the process is repeated, each time keeping track of R_i^2, until the particle is within some prescribed *very small* distance of the multiphase interface. (See Fig. 3 for an illustrative case of two-phase media with circular inclusions.) At this juncture, one must compute not only the mean time in the small neighborhood of the interface, denoted by τ_s, but the probability of crossing the interface. Both of these quantities, described fully below, are functions of $\sigma_1, \sigma_2, \ldots, \sigma_n$ and the local geometry. Thus, the expression for the effective conductivity used in practice is given by

$$\sigma_e = \frac{\langle \Sigma_i\, R_i^2 + \Sigma_j\, R_j^2\rangle}{2d\langle \Sigma_i\, \tau(R_i) + \Sigma_j\, \tau_s(R_j)\rangle}, \tag{8}$$

since $X^2 = \langle \Sigma_i\, R_i^2 + \Sigma_j\, R_j^2\rangle$. Here the summation over the

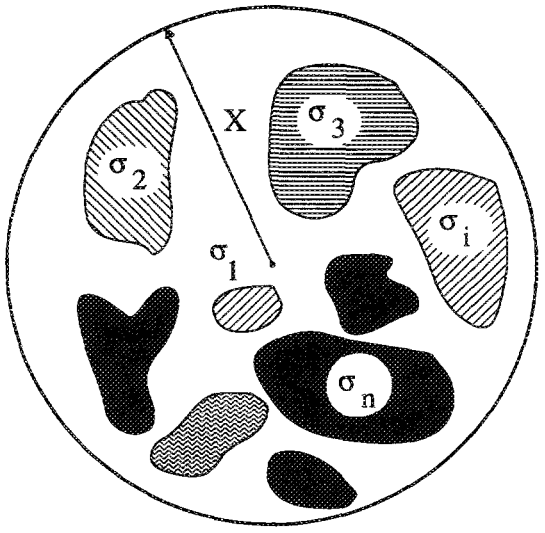

FIG. 2. General n-phase isotropic composite with conductivities $\sigma_1, \sigma_2, \ldots, \sigma_n$. The effective conductivity is σ_e. Note that the simulation technique is not limited to particulate composites as illustrated in this figure.

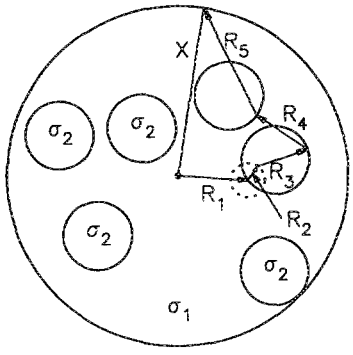

(a)

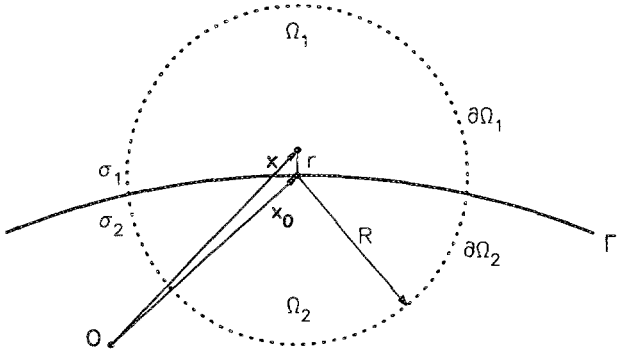

(b)

FIG. 3. (a) A two-phase medium with circular inclusions. (b) Interface boundary between the matrix of conductivity σ_1 and the circular inclusion of conductivity σ_2.

subscript i is for the random walk paths in homogeneous domains and the summation over the subscript j is for the random walk paths crossing the interface boundary.

Since each path segment, having mean square displacement R_i^2 is wholly contained in a homogeneous part of the medium, Eqs. (3) and (8) yield

$$\sigma_e = \frac{\langle \Sigma_i R_i^2 + \Sigma_j R_j^2 \rangle}{2d \langle \Sigma_i R_i^2/2d\sigma^{(i)} + \Sigma_j \tau_s(R_j) \rangle} = \frac{\langle \Sigma_i R_i^2 + \Sigma_j R_j^2 \rangle}{\langle \Sigma_i R_i^2/\sigma^{(i)} + 2d \Sigma_j \tau_s(R_j) \rangle}, \tag{9}$$

or

$$\frac{\sigma_e}{\sigma_1} = \frac{\langle \Sigma_i R_i^2/\sigma_1 + \Sigma_j R_j^2/\sigma_1 \rangle}{\langle \Sigma_i R_i^2/\sigma^{(i)} + 2d \Sigma_j \tau_s(R_j) \rangle}. \tag{10}$$

If an infinite medium is to be considered, then we have

$$\frac{\sigma_e}{\sigma_1} = \left. \frac{\langle \Sigma_i R_i^2/\sigma_1 + \Sigma_j R_j^2/\sigma_1 \rangle}{\langle \Sigma_i R_i^2/\sigma^{(i)} + 2d \Sigma_j \tau_s(R_j) \rangle} \right|_{X^2 \to \infty}. \tag{11}$$

Each term inside the brackets of Eq. (11) has dimension of time, and therefore (11) can be rewritten as

$$\frac{\sigma_e}{\sigma_1} = \left. \frac{\langle \Sigma_i \tau_1(R_i) + \Sigma_j \tau_1(R_j) \rangle}{\langle \Sigma_i \tau(R_i) + \Sigma_j \tau_s(R_j) \rangle} \right|_{X^2 \to \infty}. \tag{12}$$

Here $\tau_1(R)$ denotes the time for a random walker to make a first flight in an homogeneous sphere of radius R of conductivity σ_1. Note that for an infinite medium, the initial position of the Brownian particle is arbitrary. Equations (11) and (12) will be the basic equations used to compute the effective conductivity of random heterogeneous media.

B. Random walk crossing the interface boundary

Here we shall derive the appropriate first passage time equations (i.e., mean hitting times and probabilities) which apply in a very small neighborhood of the multiphase interface. For concreteness, we consider the interface between phase 1 and phase 2. Referring to Fig. 3 (b), the basic questions are the following:

(i) What will be the probability $p_1(\mathbf{x})$ [or $p_2(\mathbf{x})$] that the random walker initially at $\mathbf{x}$ (near $\mathbf{x}_0$, in practice), the center of an imaginary sphere of radius R, hits $\partial\Omega_1$ ($\partial\Omega_2$) for the first time without hitting $\partial\Omega_2$ ($\partial\Omega_1$)?

(ii) What will be the mean hitting time $\tau_s(\mathbf{x})$ for the random walker initially at $\mathbf{x}$ to hit $\partial\Omega (= \partial\Omega_1 \cup \partial\Omega_2)$ for the first time?

First passage time analysis[11,12] leads to the boundary-value problems given by

$$\begin{aligned} &\nabla^2 p_1 = 0 \quad \text{in } \Omega (= \Omega_1 \cup \Omega_2) \\ &p_1(\mathbf{x}) = 1 \quad \text{on } \partial\Omega_1 \\ &p_1(\mathbf{x}) = 0 \quad \text{on } \partial\Omega_2 \\ &p_1(\mathbf{x})|_1 = p_1(\mathbf{x})|_2 \quad \text{on } \Gamma \\ &\left. \frac{\partial p_1}{\partial n_1} \right|_1 = \alpha \left. \frac{\partial p_1}{\partial n_1} \right|_2 \quad \text{on } \Gamma, \end{aligned} \tag{13}$$

$$p_2(\mathbf{x}) = 1 - p_1(\mathbf{x}), \tag{14}$$

$$\begin{aligned} &\sigma_i \nabla^2 \tau_s = -1 \quad \text{in } \Omega_i \\ &\tau_s(\mathbf{x}) = 0 \quad \text{on } \partial\Omega \\ &\tau_s(\mathbf{x})|_1 = \tau_s(\mathbf{x})|_2 \quad \text{on } \Gamma \\ &\left. \frac{\partial \tau_s}{\partial n_1} \right|_1 = \alpha \left. \frac{\partial \tau_s}{\partial n_1} \right|_2 \quad \text{on } \Gamma. \end{aligned} \tag{15}$$

Here $\alpha = \sigma_2/\sigma_1$ and Γ denotes the interface surface, n_i unit outward normal from region Ω_i and $|_i$ means the approach to Γ from the region Ω_i. Note that the imaginary sphere of radius R described above is centered on interface boundary rather than on the random walker since the former lends itself to a more tractable solution.

For the nontrivial geometry as shown in Fig. 3(b), Eqs. (13)–(15) can be solved by utilizing a numerical technique such as the boundary element method. However, the local geometry seen by the random walker varies as it moves (e.g., the maximum allowable first-flight distance R can be very small if another particle is very close to the one the random walker faces). Therefore, in order to use the numerical technique such as the boundary element method, (13)–(15) must be solved for all possible geometries that the random walker can see. To avoid this difficulty, we suggest an excellent approximation to the solutions to (13)–(15) based on an analytical result for a geometry we now describe.

Consider a limiting geometry (Fig. 4) where the local radius of curvature of interface boundary around the random walker is so large compared to the maximum allowable *first-flight distance* R that the interface boundary can be considered as a straight line ($d = 2$) or a flat plane ($d = 3$). (Of course, for $d = 1$ the local radius of curvature is always infinite.) Under such conditions, Eqs. (13)–(15) are solved in terms of the relative displacement $\mathbf{x} - \mathbf{x}_0$, as

$$\begin{aligned} p_1(x) &= \frac{1}{\alpha + 1}\left[1 + \alpha\left(\frac{x}{R}\right)\right] \quad \text{for } 0 \leqslant x \leqslant R \\ &= \frac{1}{\alpha + 1}\left(1 + \frac{x}{R}\right) \quad \text{for } -R \leqslant x \leqslant 0, \end{aligned} \tag{16}$$

$$p_2(x) = 1 - p_1(x) \quad \text{for } -R \leqslant x \leqslant R, \tag{17}$$

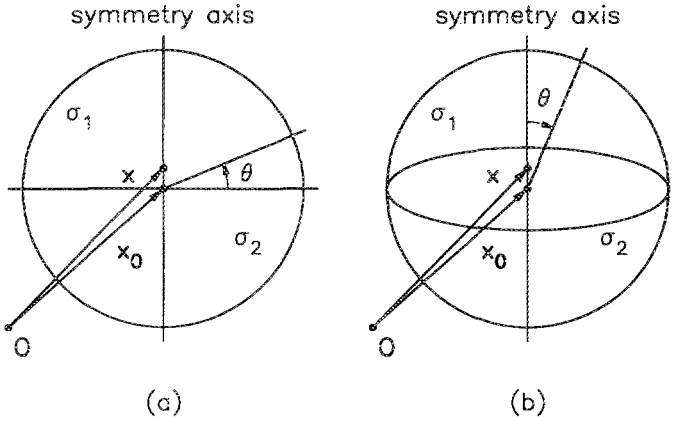

FIG. 4. Limiting geometries in d dimensions where the maximum allowable first-flight distance is so small compared to the radius of curvature of the interface that the interface can be considered to be a straight line in case of two dimensions or a flat plane in case of three dimensions. (a) $d = 2$, (b) $d = 3$.

$$\tau_s(x) = \frac{R^2}{2\sigma_1}\frac{2}{\alpha+1}\left[1-\frac{\alpha+1}{2}\left(\frac{x}{R}\right)^2+\frac{\alpha-1}{2}\left(\frac{x}{R}\right)\right]$$

for $0 \leqslant x \leqslant R$

$$= \frac{R^2}{2\sigma_1}\frac{2}{\alpha+1}\left[1-\frac{\alpha+1}{2\alpha}\left(\frac{x}{R}\right)^2+\frac{\alpha-1}{2\alpha}\left(\frac{x}{R}\right)\right]$$

for $-R \leqslant x \leqslant 0$, (18)

for the case of $d = 1$, where x is a distance from the interface boundary to the direction of the phase having conductivity σ_1,

$$p_1(r,\theta) = \frac{1}{\alpha+1}\left[1+\frac{4\alpha}{\pi}\sum_{m=0}^{\infty}\frac{1}{2m+1}\left(\frac{r}{R}\right)^{2m+1}\times\sin[(2m+1)\theta]\right] \text{ for } 0\leqslant r\leqslant R,\quad 0\leqslant\theta\leqslant\pi$$

$$= \frac{1}{\alpha+1}\left[1+\frac{4}{\pi}\sum_{m=0}^{\infty}\frac{1}{2m+1}\left(\frac{r}{R}\right)^{2m+1}\times\sin[(2m+1)\theta]\right] \text{ for } 0\leqslant r\leqslant R,\quad \pi\leqslant\theta\leqslant 2\pi, \tag{19}$$

$$p_2(r,\theta) = 1 - p_1(r,\theta) \quad \text{for } 0\leqslant r\leqslant R,\quad 0\leqslant\theta\leqslant 2\pi, \tag{20}$$

$$\tau_s(r,\theta) = \frac{R^2}{4\sigma_1}\frac{2}{\alpha+1}\left[1-\left(\frac{\alpha+1}{2}-\frac{\alpha-1}{2}\cos(2\theta)\right)\times\left(\frac{r}{R}\right)^2+\frac{\alpha-1}{2}H(r,\theta)\right]$$

for $0\leqslant r\leqslant R,\quad 0\leqslant\theta\leqslant\pi$

$$= \frac{R^2}{4\sigma_1}\frac{2}{\alpha+1}\left[1-\left(\frac{\alpha+1}{2\alpha}+\frac{\alpha-1}{2\alpha}\cos(2\theta)\right)\times\left(\frac{r}{R}\right)^2+\frac{\alpha-1}{2\alpha}H(r,\theta)\right] \tag{21}$$

for $0\leqslant r\leqslant R,\quad \pi\leqslant\theta\leqslant 2\pi$,

where

$$H(r,\theta) = \frac{2}{\pi}\sum_{m=0}^{\infty}\left(\frac{2}{2m+1}-\frac{1}{2m+3}-\frac{1}{2m-1}\right)\times\left(\frac{r}{R}\right)^{2m+1}\sin[(2m+1)\theta],$$

for the case of $d = 2$, and

$$p_1(r,\theta) = \frac{1}{\alpha+1}\left[1+\alpha\sum_{m=0}^{\infty}B_{2m+1}\times\left(\frac{r}{R}\right)^{2m+1}P_{2m+1}(\cos\theta)\right]$$

for $0\leqslant r\leqslant R,\quad 0\leqslant\theta\leqslant\frac{\pi}{2}$

$$= \frac{1}{\alpha+1}\left[1+\sum_{m=0}^{\infty}B_{2m+1}\times\left(\frac{r}{R}\right)^{2m+1}P_{2m+1}(\cos\theta)\right]$$

for $0\leqslant r\leqslant R,\quad \pi/2\leqslant\theta\leqslant\pi$, (22)

where

$$B_{2m+1} = \frac{(-1)^m(2m)!}{2^{2m+1}(m!)^2}\frac{(4m+3)}{(m+1)},$$

$$p_2(r,\theta) = 1 - p_1(r,\theta) \quad \text{for } 0\leqslant r\leqslant R,\quad 0\leqslant\theta\leqslant\pi, \tag{23}$$

$$\tau_s(r,\theta) = \frac{R^2}{6\sigma_1}\frac{2}{\alpha+1}\left[1-\left(\frac{\alpha+1}{2}+(\alpha-1)P_2(\cos\theta)\right)\times\left(\frac{r}{R}\right)^2+\frac{\alpha-1}{2}G(r,\theta)\right]$$

for $0\leqslant r\leqslant R,\quad 0\leqslant\theta\leqslant\pi/2$

$$= \frac{R^2}{6\sigma_1}\frac{2}{\alpha+1}\left[1-\left(\frac{\alpha+1}{2\alpha}-\frac{\alpha-1}{\alpha}P_2(\cos\theta)\right)\times\left(\frac{r}{R}\right)^2-\frac{\alpha-1}{2}G(r,\theta)\right] \tag{24}$$

for $0\leqslant r\leqslant R,\quad \pi/2\leqslant\theta\leqslant\pi$,

where

$$G(r,\theta) = \sum_{m=0}^{\infty}C_{2m+1}\left(\frac{r}{R}\right)^{2m+1}P_{2m+1}(\cos\theta),$$

$$C_{2m+1} = \frac{(-1)^{m+1}(2m)!}{2^{2m+1}(m!)^2}\frac{3(4m+3)}{(2m-1)(m+2)(m+1)}.$$

for the case of $d = 3$.

Here the arguments of τ_s and p_i are the components of $\mathbf{x}-\mathbf{x}_0$, where $r = |\mathbf{x}-\mathbf{x}_0|$ and θ is a direction angle in two dimensions and a spherical polar angle in three dimensions measured from a reference axis (see Fig. 4). P_n denotes the Legendre function of degree n. For simulation purposes, however, it suffices to know the solutions along the symmetry axis for $d = 2$ and $d = 3$. Thus, we have

$$p_1\left(r,\frac{\pi}{2}\right) = \frac{1}{\alpha+1}\left[1+\frac{4\alpha}{\pi}\arctan\left(\frac{r}{R}\right)\right] \quad \text{for } 0\leqslant r\leqslant R,$$

$$p_1\left(r,\frac{3\pi}{2}\right) = \frac{1}{\alpha+1}\left[1-\frac{4}{\pi}\arctan\left(\frac{r}{R}\right)\right] \quad \text{for } 0\leqslant r\leqslant R, \tag{25}$$

$$p_2\left(r,\frac{\pi}{2}\right) = 1 - p_1\left(r,\frac{\pi}{2}\right) \quad \text{for } 0\leqslant r\leqslant R,$$

$$p_2\left(r,\frac{3\pi}{2}\right) = 1 - p_i\left(r,\frac{3\pi}{2}\right) \quad \text{for } 0\leqslant r\leqslant R, \tag{26}$$

$$\tau_s\left(r,\frac{\pi}{2}\right) = \frac{R^2}{4\sigma_1}\frac{2}{\alpha+1}\left\{1-\alpha\left(\frac{r}{R}\right)^2+\frac{\alpha-1}{\pi}\times\left[\arctan\left(\frac{r}{R}\right)\left(\frac{r}{R}+\frac{R}{r}\right)^2+\left(\frac{r}{R}-\frac{R}{r}\right)\right]\right\}$$

for $0\leqslant r\leqslant R$,

$$\tau_s\left(r,\frac{3\pi}{2}\right) = \frac{R^2}{4\sigma_1}\frac{2}{\alpha+1}\left\{1-\frac{1}{\alpha}\left(\frac{r}{R}\right)^2-\frac{\alpha-1}{\pi\alpha}\times\left[\arctan\left(\frac{r}{R}\right)\left(\frac{r}{R}+\frac{R}{r}\right)^2+\left(\frac{r}{R}-\frac{R}{r}\right)\right]\right\}$$

for $0\leqslant r\leqslant R$, (27)

for the case of $d = 2$, and

$$p_1(r,0) = \frac{1}{\alpha+1}\left[1+\alpha\sum_{m=0}^{\infty}B_{2m+1}\left(\frac{r}{R}\right)^{2m+1}\right]$$

for $0\leqslant r\leqslant R$, (28)

$$p_1(r,\pi)=\frac{1}{\alpha+1}\left[1-\sum_{m=0}^{\infty}B_{2m+1}\left(\frac{r}{R}\right)^{2m+1}\right]$$

for $0\leqslant r\leqslant R$,

$$p_2(r,0)=1-p_1(r,0) \quad \text{for } 0\leqslant r\leqslant R,$$

$$p_2(r,\pi)=1-p_1(r,\pi) \quad \text{for } 0\leqslant r\leqslant R, \tag{29}$$

$$\tau_s(r,0)=\frac{R^2}{6\sigma_1}\frac{2}{\alpha+1}\left[1-\frac{3\alpha-1}{2}\left(\frac{r}{R}\right)^2+\frac{\alpha-1}{2}\sum_{m=0}^{\infty}C_{2m+1}\left(\frac{r}{R}\right)^{2m+1}\right]$$

for $0\leqslant r\leqslant R$,

$$\tau_s(r,\pi)=\frac{R^2}{6\sigma_1}\frac{2}{\alpha+1}\left[1+\frac{\alpha-3}{2\alpha}\left(\frac{r}{R}\right)^2-\frac{\alpha-1}{2\alpha}\sum_{m=0}^{\infty}C_{2m+1}\left(\frac{r}{R}\right)^{2m+1}\right]$$

for $0\leqslant r\leqslant R$, (30)

where

$$B_{2m+1}=\frac{(-1)^m(2m)!}{2^{2m+1}(m!)^2}\frac{(4m+3)}{(m+1)},$$

$$C_{2m+1}=\frac{(-1)^{m+1}(2m)!}{2^{2m+1}(m!)^2}\frac{3(4m+3)}{(2m-1)(m+2)(m+1)},$$

for the case of $d=3$. Of course, for $d=1$, we still have Eqs. (16)–(18).

It is noteworthy that if a random walker starts from the center of a d-dimensional sphere at $\mathbf{x}_0$ (i.e., $x=0$ for $d=1$ and $r=0$ for $d=2$ and 3), then we have the simple relations:

$$p_1=1/(\alpha+1), \tag{31}$$

$$p_2=\alpha/(\alpha+1), \tag{32}$$

$$\tau_s/\tau_1=2/(\alpha+1), \tag{33}$$

where $\tau_1=R^2/2d\sigma_1$ is the mean hitting time for the homogeneous sphere of conductivity σ_1. The expressions (31)–(33) provide a basis for us to obtain the simple approximations to the solutions of (13)–(15) for the general geometry illustrated in Fig. 3(b) in which the interface has some finite curvature. For a random walker initially on the interface at position $\mathbf{x}_0$ as in Fig. 4, the probability of reaching a unit surface area (or unit arc length in two dimensions) of a boundary segment $\partial\Omega_i$ is proportional to the conductivity of the region adjacent to that boundary. Applying this reasoning for the general geometry depicted in Fig. 4, the probability $p_1(\mathbf{x}_0)$ $[p_2(\mathbf{x}_0)]$ that a random walker at a point $\mathbf{x}_0$ on the interface, hits $\partial\Omega_1$ $(\partial\Omega_2)$ for the first time without hitting $\partial\Omega_2$ $(\partial\Omega_1)$, will be

$$p_1(\mathbf{x}_0)=\frac{A_1\sigma_1}{A_1\sigma_1+A_2\sigma_2}=\frac{A_1}{A_1+A_2\alpha}, \tag{34}$$

$$p_2(\mathbf{x}_0)=1-p_1(\mathbf{x}_0)=\frac{A_2\alpha}{A_1+A_2\alpha}, \tag{35}$$

where A_1 and A_2 are the surface areas of $\partial\Omega_1$ and $\partial\Omega_2$, respectively.

The mean hitting time can also be obtained using similar arguments. For each Brownian trajectory which first strikes $\partial\Omega$ from a point at $\mathbf{x}_0$ at the interface (see Fig. 4), the probability that the diffusing particle visits a volume element will be proportional to the local conductivity of that volume element. Furthermore, the time spent for each local random walk is inversely proportional to the local conductivity. Therefore, for the position $\mathbf{x}_0$ on the interface, the mean hitting time $\tau_s(\mathbf{x}_0)$ will be

$$\tau_s(\mathbf{x}_0)=\frac{V_1\sigma_1}{V_1\sigma_1+V_2\sigma_2}\tau_1+\frac{V_2\sigma_2}{V_1\sigma_1+V_2\sigma_2}\frac{\tau_1}{\alpha}=\frac{V_1+V_2}{V_1+\alpha V_2}\tau_1. \tag{36}$$

If $|\mathbf{x}-\mathbf{x}_0|/R\ll 1$ along the symmetry axis, we can conjecture that the solution to (13)–(15), with the aid of (25)–(30) and (34)–(36) can be approximated by

$$p_1\left(r,\frac{\pi}{2}\right)=\frac{A_1}{A_1+\alpha A_2}\left[1+\frac{4\alpha}{\pi}\arctan\left(\frac{r}{R}\right)\right]$$

for $0\leqslant r\leqslant R$,

$$p_1\left(r,\frac{3\pi}{2}\right)=\frac{A_1}{A_1+\alpha A_2}\left[1-\frac{4}{\pi}\arctan\left(\frac{r}{R}\right)\right]$$

for $0\leqslant r\leqslant R$, (37)

$$p_2\left(r,\frac{\pi}{2}\right)=1-p_1\left(r,\frac{\pi}{2}\right) \quad \text{for } 0\leqslant r\leqslant R,$$

$$p_2\left(r,\frac{3\pi}{2}\right)=1-p_1\left(r,\frac{3\pi}{2}\right) \quad \text{for } 0\leqslant r\leqslant R, \tag{38}$$

$$\tau_s\left(r,\frac{\pi}{2}\right)=\frac{R^2}{4\sigma_1}\frac{V_1+V_2}{V_1+\alpha V_2}\left\{1-\alpha\left(\frac{r}{R}\right)^2+\frac{\alpha-1}{\pi}\times\left[\arctan\left(\frac{r}{R}\right)\left(\frac{r}{R}+\frac{R}{r}\right)^2+\left(\frac{r}{R}-\frac{R}{r}\right)\right]\right\}$$

for $0\leqslant r\leqslant R$,

$$\tau_s\left(r,\frac{3\pi}{2}\right)=\frac{R^2}{4\sigma_1}\frac{V_1+V_2}{V_1+\alpha V_2}\left\{1-\frac{1}{\alpha}\left(\frac{r}{R}\right)^2-\frac{\alpha-1}{\pi\alpha}\times\left[\arctan\left(\frac{r}{R}\right)\left(\frac{r}{R}+\frac{R}{r}\right)^2+\left(\frac{r}{R}-\frac{R}{r}\right)\right]\right\}$$

for $0\leqslant r\leqslant R$, (39)

for the case of $d=2$, and

$$p_1(r,0)=\frac{A_1}{A_1+\alpha A_2}\left[1+\alpha\sum_{m=0}^{\infty}B_{2m+1}\left(\frac{r}{R}\right)^{2m+1}\right]$$

for $0\leqslant r\leqslant R$,

$$p_1(r,\pi)=\frac{A_1}{A_1+\alpha A_2}\left[1-\sum_{m=0}^{\infty}B_{2m+1}\left(\frac{r}{R}\right)^{2m+1}\right]$$

for $0\leqslant r\leqslant R$, (40)

$$p_2(r,0)=1-p_1(r,0) \quad \text{for } 0\leqslant r\leqslant R,$$

$$p_2(r,\pi)=1-p_1(r,\pi) \quad \text{for } 0\leqslant r\leqslant R, \tag{41}$$

$$\tau_s(r,0)=\frac{R^2}{6\sigma_1}\frac{V_1+V_2}{V_1+\alpha V_2}\left[1-\frac{3\alpha-1}{2}\left(\frac{r}{R}\right)^2+\frac{\alpha-1}{2}\sum_{m=0}^{\infty}C_{2m+1}\left(\frac{r}{R}\right)^{2m+1}\right]$$

for $0\leqslant r\leqslant R$,

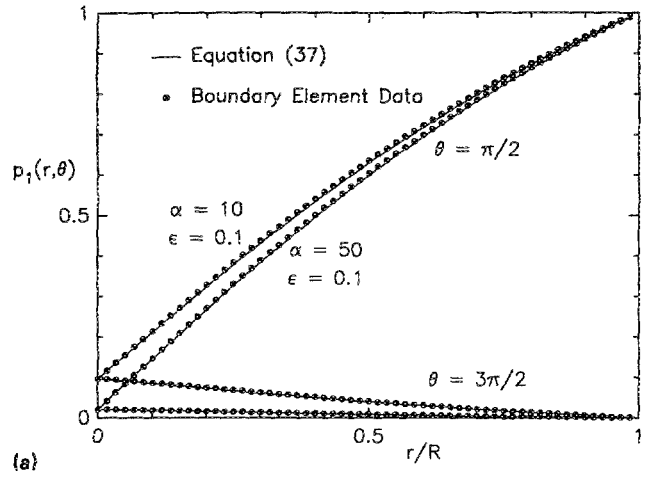

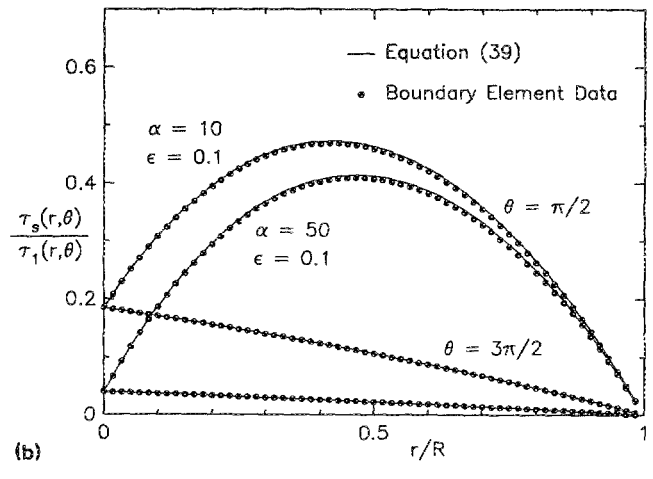

FIG. 5. Comparison of the analytical expressions (37) and (39) (solid lines) and the boundary element data (circles) for $\alpha = 10$ and 50 and $\epsilon = 0.1$. Here ϵ is the dimensionless ratio of the first flight distance R to the radius of the curvature of the interface. (a) Probability of jumping in phase 1, p_1; upper curves corresponds to $\theta = \pi/2$ and lower curves corresponds to $\theta = 3\pi/2$. (b) Mean hitting time, τ_s (where τ_1 is the mean hitting time for the homogeneous material of conductivity σ_1); upper curves corresponds to $\theta = \pi/2$ and lower curves corresponds to $\theta = 3\pi/2$.

$$\tau_s(r,\pi) = \frac{R^2}{6\sigma_1}\frac{V_1+V_2}{V_1+\alpha V_2}\left[1+\frac{\alpha-3}{2\alpha}\left(\frac{r}{R}\right)^2 - \frac{\alpha-1}{2\alpha}\sum_{m=0}^{\infty} C_{2m+1}\left(\frac{r}{R}\right)^{2m+1}\right]$$

for $0 \leqslant r \leqslant R$, (42)

where

$$B_{2m+1} = \frac{(-1)^m(2m)!}{2^{2m+1}(m!)^2}\frac{(4m+3)}{(m+1)},$$

$$C_{2m+1} = \frac{(-1)^{m+1}(2m)!}{2^{2m+1}(m!)^2}\frac{3(4m+3)}{(2m-1)(m+2)(m+1)},$$

for the case of $d = 3$.

In order to test the validity and accuracy of relations (37)–(42), we solved Eqs. (13)–(15) using the boundary element method for various radii of curvatures of the interface boundary for two-dimensional media. We specifically studied the cases $\epsilon = 0.01, 0.02, \ldots, 0.1$ where ϵ is the ratio of the first flight distance R to the radius of curvature of the interface boundary. In Fig. 5, we compare the boundary element results along the symmetry axis with the analytical relations (37)–(39) for the worst case of $\epsilon = 0.1$ (in which the maximum deviations from the analytical relations (37)–(39) occur) when $\alpha = 10$ and 50. The agreement is seen to be excellent, i.e., on the scale of our figure, the numerical and analytical results are indistinguishable even at the worst case of $\epsilon = 0.1$. Therefore, application of relations (37)–(42) near the multiphase interface should yield highly accurate results for τ_s and p_i.

C. Interface equations for perfectly insulating phase relative to a connected phase

Consider the general case where phase 2 is perfectly insulating relative to a *connected* phase 1 ($\alpha = 0$). Phase 2 may be disconnected or connected for $d = 3$, but is always disconnected for $d < 3$. If $\alpha = 0$, then Eqs. (37) to (42) can be successfully used without any difficulty. Consider a random walker initially at the arbitrary location in the system. It is clear that if the random walker is in the insulating phase 2 (i.e., $\alpha = 0$), it will stay there forever and once the random walker is in the noninsulating phase (phase 1), it can never enter into phase 2. This can be easily seen from Eqs. (37), (38), (40), and (41), where it is found that $p_1 = 1$, and $p_2 = 0$ for $d = 2$ and 3. Furthermore, Eqs. (39) and (42) yield, for $\alpha = 0$.

$$\tau_s\left(r,\frac{\pi}{2}\right) = \frac{R^2}{4\sigma_1}\frac{V_1+V_2}{V_1}\left\{1-\frac{1}{\pi}\left[\arctan\left(\frac{r}{R}\right)\times\left(\frac{r}{R}+\frac{R}{r}\right)^2+\left(\frac{r}{R}-\frac{R}{r}\right)\right]\right\}, \quad \text{for } 0 \leqslant r \leqslant R, \tag{43}$$

for the case of $d = 2$, and

$$\tau_s(r,0) = \frac{R^2}{6\sigma_1}\frac{V_1+V_2}{V_1}\left[1+\frac{1}{2}\left(\frac{r}{R}\right)^2 - \frac{1}{2}\sum_{m=0}^{\infty} C_{2m+1}\left(\frac{r}{R}\right)^{2m+1}\right], \quad \text{for } 0 \leqslant r \leqslant R, \tag{44}$$

where

$$C_{2m+1} = \frac{(-1)^{m+1}(2m)!}{2^{2m+1}(m!)^2}\frac{3(4m+3)}{(2m-1)(m+2)(m+1)}$$

for the case of $d = 3$. Note that since the random walker is forbidden from entering the insulating phase, $\tau_s(r,3\pi/2)$ (for $d = 2$) and $\tau_s(r,\pi)$ (for $d = 3$) are not considered.

It is worthwhile to note that one needs to be careful in computing the mean square displacement of the random walkers [as in Eq. (8)] for $\alpha = 0$. In order to compute the mean square displacement of the random walkers, the sum of the square displacements should be averaged over all random walkers (including the ones initially trapped in phase 2), *not only* the random walkers that can freely move in

phase 1. If we have M such freely moving random walkers and since the probability of finding a random walker initially located in phase i will be simply ϕ_i, then the number of random walkers over which we should average to compute the mean square displacement will be M/ϕ_1. Thus, if the right-hand side of Eq. (8) [and hence Eqs. (9)–(12)] is computed over only the freely moving random walkers, then we have to multiply this result by a factor of ϕ_1.

Note that this relation can be applied for any microgeometry including the cases in which both phases are connected (e.g., as can be seen in a sandstone). Equation (44) can also be employed in instances where one has an infinitely conducting but connected phase relative to another connected phase since the case of a perfectly insulating phase 2 relative to phase 1 ($\sigma_2/\sigma_1 = 0$) is equivalent to an infinitely conducting phase 1 relative to phase 2 ($\sigma_1/\sigma_2 = \infty$).

D. Interface equations for infinitely conducting phase relative to a connected phase

Consider the general case where phase 2 is infinitely conducting relative to a *connected* phase 1 ($\alpha = \infty$). Phase 2 may be disconnected or connected in three dimensions, but must be disconnected in lower dimensions. When phase 2 is also connected, we can use the algorithm described in Sec. II C. Therefore, we consider only the case where phase 2 is disconnected. If $\alpha = \infty$, Eqs. (40)–(42) yield trivial answers: $p_1(r) = 0$, $p_2(r) = 1$, and $\tau_s(r) = 0$. This implies that the random walker initially at the interface boundary between phase 1 and phase 2 will always be trapped in the infinitely conducting phase and thus can never escape from there. Moreover, Eq. (42) implies this process requires no time. This is undesirable from a simulation standpoint and hence one needs to modify the random walk algorithm under such conditions. We first describe the appropriate equations for phase 2 composed of d-dimensional spherical inclusions and subsequently generalize our arguments for arbitrary *microgeometries*.

Consider the random walker initially at $\mathbf{x}_0$, the center of the spherical inclusion of radius a as shown in Fig. 6. Construct a concentric sphere of radius R around the inclusion such that the concentric shell of thickness $(R-a)$ contains only phase 1. The mean hitting time for striking the surface $\partial\Omega$ of the sphere of radius R is obtained by solving Eq. (15) and is given by

$$\tau_s(\mathbf{x}_0) = \frac{R^2}{2d\sigma_1}\left(1 - \frac{a^2}{R^2}\right). \tag{45}$$

Since it will not take any time for the random walker initially at the interface boundary y to hit $\mathbf{x}_0$, the mean hitting time to strike $\partial\Omega$ from the position y is

$$\tau_s(\mathbf{y}) = \frac{R^2}{2d\sigma_1}\left(1 - \frac{a^2}{R^2}\right) \quad \text{on } \Gamma. \tag{46}$$

For a random walker initially at some normal position vector z measured with respect to Γ, then we have

$$\tau_s(\mathbf{x}) = \frac{R^2}{2d\sigma_1}\left(1 - \frac{(r+a)^2}{R^2}\right), \quad 0 \leqslant r \leqslant \delta(R-a), \tag{47}$$

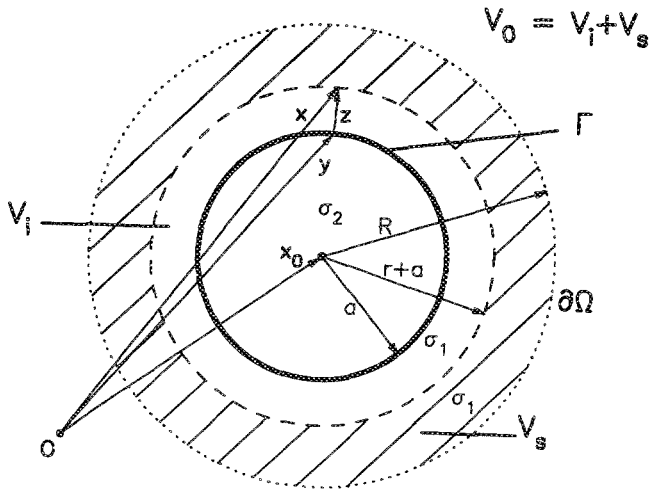

FIG. 6. A sample geometry for the case of $\alpha = \sigma_2/\sigma_1 = \infty$ for the illustrative case of a spherical inclusion centered at $\mathbf{x}_0$. Here V_i is the volume of the sphere of radius a (of conductivity σ_2) plus the volume of the imaginary concentric inner shell of thickness $r = |\mathbf{z}|$, $\mathbf{z} = \mathbf{x} - \mathbf{y}$, (of conductivity σ_1), and V_s is the volume of the imaginary concentric outer shell of thickness $[R - (r+a)]$ (of conductivity σ_1). Furthermore, V_o is the sum of V_i and V_s, $\partial\Omega$ denotes the outer surface defined by x, and Γ denotes the interface boundary defined by y.

where $r = |\mathbf{z}|$ and δ is a prescribed small number. Note that we only have to consider the random walk in the (connected) phase 1 since once it touches the interface boundary Γ, it will jump to $\partial\Omega$ spending an amount of time given by (47).

For arbitrary-shaped inclusions (phase 2), Eq. (47) needs further modification. Construct concentric shells around this inclusion as in the instance of the spherical inclusion above. Noting that $(r+a)^2/R^2 \propto (V_i/V_o)^{2/d}$ where V_i and V_o are the volume of the inclusion plus its surrounding inner concentric shell (corresponding to the concentric shell of thickness r in the case of the spherical inclusion), and volume of the inclusion plus its surrounding outer concentric shell (corresponding to the concentric shell of thickness $(R-a)$ in the case of the spherical inclusion), respectively (see Fig. 6), Eq. (47) generalizes as

$$\tau_s(\mathbf{x}) = \tau_1(1 - V_i^{2/d}/V_o^{2/d}). \tag{48}$$

Here τ_1 is the mean hitting time for the random walker initially at the center of mass of the homogeneous region of volume V and conductivity σ_1 to first strike the surface of this volume. τ_1 for an arbitrary-shaped region can be easily determined by solving the governing equation (2) by use of any common numerical technique (e.g., boundary element method). With Eqs. (47) and (48), the relation (12) can be used.

We provide an example to show that the above algorithm yields the exact effective conductivity. Consider a one-dimensional two-phase regular array (e.g., regular arrangement of parallel slabs which alternate between phase 1 and phase 2 materials with volume fractions ϕ_1 and ϕ_2, respectively) (see Fig. 7). Let $\alpha = \infty$ and the distance between two nearest phase 2 slabs be unity. For such a geometry we

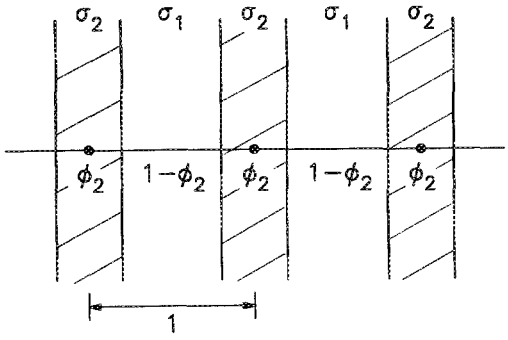

FIG. 7. One-dimensional two-phase regular array.

know that $\sigma_e/\sigma_1 = 1/(1-\phi_2)$. Since it takes no time for a Brownian particle at the interface to walk to the center of the infinitely conducting slab, then once it hits the interface the ensuing random walk can be considered to be a simple random walk with a constant step size of unity spending (on average) an amount of time at each step given by

$$\tau_s = \frac{(1-\phi_2/2)^2}{2\sigma_1}\left(1-\frac{(\phi_2/2)^2}{(1-\phi_2/2)^2}\right)$$
$$= \frac{1}{2\sigma_1}(1-\phi_2). \tag{49}$$

Therefore, using (12), we find the exact result

$$\frac{\sigma_e}{\sigma_1} = \lim_{N\to\infty} \frac{\langle t_1 + \sum^N (1/2\sigma_1)\rangle}{\langle t_e + \sum^N (1-\phi_2)/2\sigma_1\rangle}$$
$$= 1/(1-\phi_2). \tag{50}$$

Here t_1 and t_e are the times for a random walker at an arbitrary initial location to reach any interface for the first time in an homogeneous medium of conductivity σ_1 and in the composite medium, respectively, and N is the number of steps.

III. SIMULATION DETAILS AND RESULTS

Here we apply the Brownian motion formulation to compute the effective transverse conductivity σ_e of two-phase composites composed of an *equilibrium* distribution of infinitely long, oriented, hard cylinders of conductivity σ_2 in a matrix of conductivity σ_1. We consider the cases $\alpha = \sigma_2/\sigma_1 = 10$, 50, and ∞. Since these results combined with the phase-interchange theorem[13] yield corresponding results for the effective conductivity when $\alpha = 0.1, 0.02$, and 0, respectively, we do not need to use the simulation technique to obtain results for insulating cylinders ($\alpha < 1$). To assess the accuracy of the method, we also compute σ_e for the idealized microgeometry of a square array of infinitely long, oriented cylinders of conductivity σ_2 in a matrix of conductivity σ_1 since its solution is known exactly numerically.[14] Before presenting these simulation results, we first describe the simulation procedure in some detail.

A. Simulation details

Obtaining the effective conductivity σ_e from computer simulations is a two-step process: (i) First, one must generate realizations of the random heterogeneous medium; (ii) Second, employing the Brownian motion algorithm, one determines the effective conductivity for each realization (using many random walkers) and then average over a sufficiently large number of realizations to obtain σ_e.

In order to generate equilibrium configurations of hard circular disks (parallel circular cylinders) at area (volume) fraction ϕ_2, we employ a conventional Metropolis algorithm.[15] N disks of radius a are initially placed on the lattice sites of a square array in a square unit cell. The unit cell is surrounded by periodic images of itself. Each disk is then moved by a small distance to a new position which is accepted or rejected according to whether or not disks overlap. This process is repeated until equilibrium is achieved. In our simulations $N = 100$ and each disk is moved 200 times before sampling for equilibrium realizations. In order to ensure that equilibrium is achieved, we determine the pressure (proportional to the radial distribution function at contact) as a function $\phi_2 = N\pi a^2$. The pressures so obtained were found to be in excellent agreement with previous theoretical and numerical calculations (see Ref. 16 and references therein). Our simulations are carried out for a wide range of ϕ_2, i.e., $0 \leqslant \phi_2 \leqslant 0.7$; $\phi_2 = 0.7$ corresponds to a value slightly higher than the hard-disk phase transition.[17]

The essence of the Brownian motion algorithm has been described in Sec. II. Here we need to be more specific about the conditions under which the Brownian particle is considered to be in the small neighborhood of the interface and hence when the mean time τ_s, and probabilities p_1 and p_2 need to be computed. An imaginary thin concentric shell of radius $a(1+\delta_1)$ is drawn around each disk of radius a. If a Brownian particle enters this thin shell, then we employ the first passage time equations (37)–(39), or (47). The radius of this first flight R is virtually always taken to be the distance to the next nearest neighboring disk or some prescribed smaller distance $\delta_2 a$. However, in the *rare* instances in which two or more interface boundaries are very close together, R would be less than $\delta_1 a$, and hence it would take a large amount of computation time for such a random walker to move even a small distance. Therefore in these rare instances, we take $R = \delta_2 a$ and instead of using Eqs. (37)–(39), or (47), we use Eqs. (51) and (52) which when generalized to n-phase media are given by

$$p_i(\mathbf{x}) = A_i\sigma_i / \sum_{j=1}^{n} A_j\sigma_j, \tag{51}$$

for the probability of a random walker jumping into phase i ($i = 1,2,\ldots,n$), and

$$\tau_s(\mathbf{x}) = \tau_1\left(\sum V_i\sigma_i / \sum V_i\sigma_i\right), \tag{52}$$

for the mean hitting time. Here A_i and V_i are the total surface area and the total volume of ith phase, respectively.

Note that since the separations between these interface boundaries are very small and the distance from the random walker to the nearest interphase boundary is also very small, then it will not make any significant difference to center the first flight sphere at x (the position of the random walker) instead of the nearest interface boundary (as in the preponderance of situations—see Sec. II) and hence using Eqs. (51) and (52) should still give accurate results. Furthermore, note that such infrequent events will make a very small contribution to the total mean time for the entire random walk.

After a sufficiently large *total* mean square displacement, Eq. (12) is then employed to yield the effective conductivity for each Brownian trajectory and each realization. Many different Brownian trajectories are considered per realization. The effective conductivity σ_e is finally determined by averaging the conductivity over all realizations. Finally, note that so-called Grid method[18] is used to reduce the computation time needed to check if the walker is near a disk. It enables one to check for disks in the immediate neighborhood of the walker instead of checking each disk.

B. Square array results

In order to assess the accuracy of our Brownian motion algorithm, we have computed σ_e for a square array of hard, oriented cylinders with $\alpha = 10$, 50, and ∞ since exact numerical data are already available for this model.[14] Here we have taken $\delta_1 = 0.0001$ and $\delta_2 = 0.01$. We employed 2000 to 6000 random walks, and have let the dimensionless total mean square displacement X^2/a^2 vary from 10 to 100, depending on the value of ϕ_2 and α. A wide range of cylinder volume fraction values were considered. Figure 8 compares our simulation results with the exact data of Ref. 14. It is quite apparent that our simulation results are in excellent agreement with the previous exact numerical results, for both finite and infinite values of α. The maximum error for the reported values was less than 1%.

We also determined the conductivity for $\alpha = \infty$ and a volume fraction $\phi_2 = 0.78$ (see Fig. 8), which is slightly below the percolation threshold of $\phi_2 = \pi/4$ (i.e., at the close-packing value). The prediction was again within 1% of the exact result[14] of $\sigma_e/\sigma_1 = 35.9$ for this case, indicating that our procedure can be employed to study percolation behavior.

Our calculations were carried out on a VAX station 3100 and on a CRAY Y-MP.

C. Equilibrium hard-cylinder results

Here we report computer simulation data for the effective transverse conductivity σ_e of equilibrium distributions of infinitely long, oriented hard cylinders for $\alpha = 10$, 50, and ∞ and for $0 < \phi_2 \leqslant 0.7$. Tables I and II and Figs. 9 and 10 summarize our findings for the scaled conductivity σ_e/σ_1. Included in the tables and figures is the rigorous four-point lower bound on σ_e/σ_1 due to Milton[19] which depends upon a microstructural parameter ζ_2. Torquato and Lado[20] evaluated ζ_2 exactly through second order in ϕ_2:

$$\zeta_2 = (\phi_2/3) - 0.05707\phi_2^2 + O(\phi_2^3). \tag{53}$$

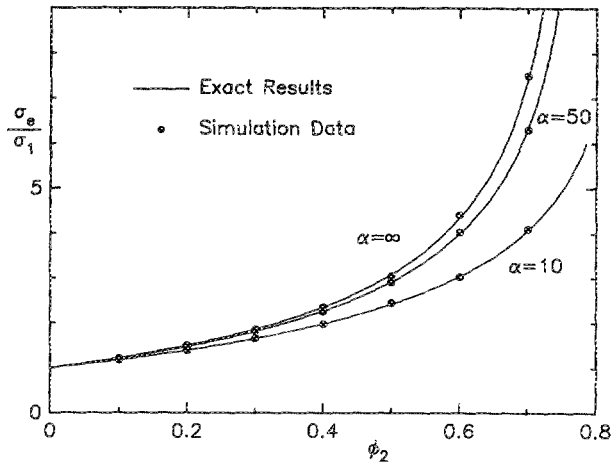

FIG. 8. Scaled transverse effective conductivity σ_e/σ_1 of a square array of cylinders in a matrix for $\alpha = \sigma_2/\sigma_1 = 10$, 50, and ∞. Solid lines are the exact numerical results obtained from Ref. 14 and the circles are our simulation data. Note that we also computed σ_e/σ_1 for the case $\alpha = \infty$ and a volume fraction of $\phi_2 = 0.78$, which is slightly below the percolation threshold of $\phi_2 = \pi/4 \simeq 0.7854$ (not shown here). The prediction is again in excellent agreement with the exact result.[14]

The simulation results of Sangani and Yao[21] and of Miller and Torquato[22] demonstrate that this expression is a very good approximation to ζ_2 for $0 \leqslant \phi_2 \leqslant 0.7$. Thus, Eq. (53) is used to compute Milton's lower bound which incorporates higher-order microstructural information via a four-point correlation function. Note that we do not give the corresponding four-point upper bound since the *lower* bound will provide the better estimate of σ_e for $\alpha > 1$.[20]

Employing our results for $\alpha = 10$, 50, and ∞ and the phase-interchange theorem[23]

$$\sigma_e(\sigma_1,\sigma_2)\sigma_e(\sigma_2,\sigma_1) = \sigma_1\sigma_2, \tag{54}$$

we can get corresponding results for $\alpha = 0.1$, 0.02, and 0, respectively. In Fig. 11 we give σ_e/σ_1 for the case of $\alpha = 0$ using our data for $\alpha = \infty$. Included in Fig. 11 is Milton's four-point *upper* bound on σ_e/σ_1 which also depends on ζ_2. The corresponding lower bound for $\alpha = 0$ vanishes.

TABLE I. Brownian motion simulation data for the scaled conductivity σ_e/σ_1 of equilibrium distributions of infinitely long, hard, oriented circular cylinders of conductivity σ_2 in a matrix of conductivity σ_1 for $\alpha = \sigma_2/\sigma_1 = 10$ and 50 at $\phi_2 = 0.2$, 0.4, and 0.6. Included in the table is Milton's four-point lower bound[a] using the microstructural parameter $\zeta_2 = \phi_2/3 - 0.05707\phi_2^2$ as obtained by Torquato and Lado.[b]

	$\alpha = 50$		$\alpha = 10$	
ϕ_2	σ_e/σ_1 Simulation results	σ_e/σ_1 Four-point lower bound	σ_e/σ_1 Simulation results	σ_e/σ_1 Four-point lower bound
0.2	1.41	1.41	1.54	1.51
0.4	2.07	2.05	2.48	2.41
0.6	3.14	3.13	4.53	4.23

[a] Reference 19.
[b] Reference 20.

TABLE II. Brownian motion simulation data for the scaled conductivity σ_e/σ_1 of equilibrium distributions of infinitely long, oriented, hard cylinders which are perfectly conducting relative to the matrix ($\alpha = \infty$) at $\phi_2 = 0.1, 0.3, 0.5$, and 0.7. Included in the table in Milton's four-point lower bound[a] using the microstructural parameter $\zeta_2 = \phi_2/3 - 0.05707\phi_2^2$ as obtained by Torquato and Lado.[b]

	$\alpha = \infty$	
ϕ_2	σ_e/σ_1 Simulation results	σ_e/σ_1 Four-point lower bound
0.1	1.23	1.23
0.3	1.97	1.95
0.5	3.59	3.36
0.7	8.29	6.87

[a] Reference 19.
[b] Reference 20.

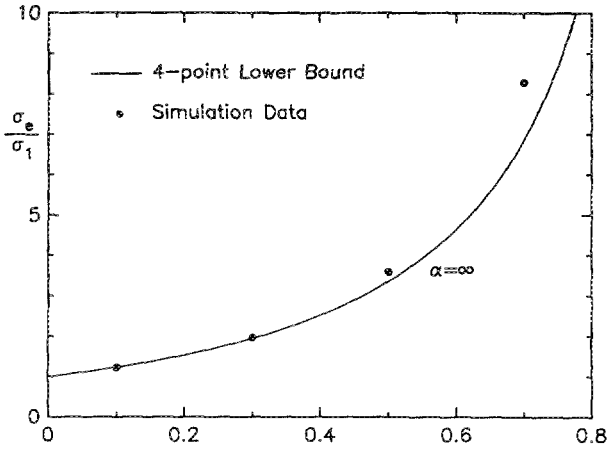

FIG. 10. As in Fig. 9, except for $\alpha = \infty$.

In our simulations, we have taken $\delta_1 = 0.0001$ and $\delta_2 = 0.01$. We considered 200 to 600 equilibrium realizations and 100 random walks per realization, and have let the dimensionless total mean square displacement X^2/a^2 vary from 10 to 1000, depending on the values of ϕ_2 and α. Compared to previous simulation techniques, the Brownian motion simulation algorithm yields accurate values of σ_e (within 2%), especially for such large random systems, with a reasonably fast execution time (e.g., on average the calculations for $\alpha = 50$ and ∞, respectively, required 2.5 and 1.2 CPU hours on a CRAY Y-MP). It is important to emphasize, however, that reduction of the number of realizations by an order of magnitude reduces the computing time proportionally but with little loss in accuracy (i.e., approximately 5% accuracy level). It is noteworthy that even at high values of the volume fraction ϕ_2, σ_e/σ_1 can be estimated accurately with relatively small computation cost. Most of the computational time is spent generating Brownian trajectories and, hence, increasing the system size (i.e., increasing N) adds negligibly small computational cost.

It should be mentioned that for the case $\alpha = 50$, Durand and Ungar[23] computed σ_e/σ_1 for the same model using a boundary element method for a unit cell containing only 16 particles. Our data are very close to theirs except at the highest area (volume) fractions where our results are slightly higher than theirs. Sangani and Yao[21] using a different technique calculated σ_e/σ_1 for the same model for the special case of infinitely conducting cylinders ($\alpha = \infty$). We find

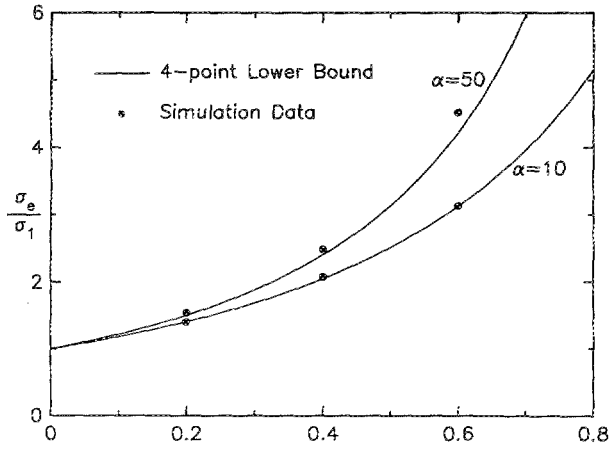

FIG. 9. Scaled transverse effective conductivity σ_e/σ_1 of an equilibrium distribution of hard cylinders in a matrix for $\alpha = \sigma_2/\sigma_1 = 10$ and 50. Solid lines are four-point lower bounds (see Ref. 19) and the circles are our simulation data.

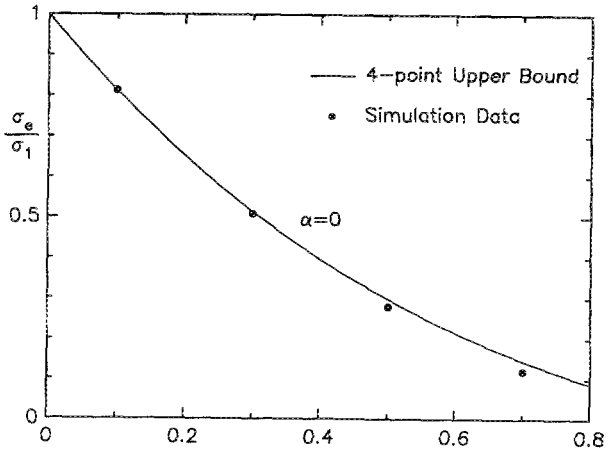

FIG. 11. Scaled transverse effective conductivity σ_e/σ_1 of an equilibrium distribution of hard cylinders in a matrix for $\alpha = \sigma_2/\sigma_1 = 0$. Solid line is the four-point upper bound (see Ref. 19) and the circles are obtained from the data for the case of $\alpha = \infty$ and the phase-interchange theorem, Eq. (54).

that our data are essentially the same as theirs at low densities ($\phi_2 = 0.1$ and 0.3) but somewhat higher than theirs at high densities ($\phi_2 = 0.5$ and 0.7). The differences are probably due to the smaller system size used in Ref. 21. Unlike the Brownian motion simulation technique, the computation time for the methods of Refs. 21 and 23 increase significantly as the system size increases.

It is useful to comment on the sources of errors. Besides statistical errors, the major sources of errors are: (i) the finite number of random walks employed and (ii) the finite length of the random walks. The number of walkers and the walker lengths employed (described above) are sufficiently large to ensure that our estimations of the effective conductivity of random arrays of cylinders are on average accurate to within 2%.

IV. CONCLUSIONS

The general Brownian motion simulation technique of Torquato and Kim[10] has been applied and extended to compute the effective conductivity σ_e of general isotropic, d-dimensional, n-phase heterogeneous media having arbitrary phase conductivities. The appropriate first passage time equations have been derived to treat such a composite media with arbitrary microgeometry. Thus the procedure can be employed to determine the conductivity of particulate composites, such as dispersions of inclusions (e.g., nonoverlapping particles) as well as physically connected particles (e.g., overlapping particles), and general heterogeneous media that are not composed of particles. To illustrate the method, we have computed the transverse effective conductivity of a heterogeneous medium consisting of an equilibrium distribution of infinitely long, oriented, hard cylinders of conductivity σ_2 in a matrix of conductivity σ_1 for a wide range of ϕ_2 (cylinder volume fraction) and for several values of the conductivity ratio $\alpha = \sigma_2/\sigma_1$. To our knowledge, this represents the most comprehensive computational study of σ_e for this useful model of a fiber-reinforced composite. The Brownian motion simulation technique is shown to yield σ_e accurately with a comparatively fast execution time.

Although random-walk techniques have recently been used to predict effective properties associated with diffusional transport in continuum (off-lattice) models,[24–26] to our knowledge, this is the first time that the effective conductivity has been determined using first passage time analysis. Previous studies[24–26] have simulated the detailed zig-zag motion of the random walker with sufficiently small step size. The computational advantages of first passage time algorithms over simulating the zig-zag motion in detail have been described by Torquato and Kim.[10]

Finally we note that the present algorithm has been applied to determine the effective conductivity of a three-dimensional suspension of impenetrable spheres,[27] a useful model for which there are still very few simulation data.

ACKNOWLEDGMENTS

The authors gratefully acknowledge the support of the Office of Basic Energy Sciences, U.S. Department of Energy, under Grant No. DE-FG05-86ER13482. Some computer resources (CRAY Y-MP) were supplied by the North Carolina Supercomputer Center funded by the State of North Carolina.

[1] J. C. Maxwell, *Treatise on Electricity and Magnetism* (Clarendon, Oxford, 1873).
[2] Lord Rayleigh, Philos. Mag. **34**, 481 (1892).
[3] A. Einstein, Ann. Phys. **19**, 289 (1906).
[4] S. Torquato, Rev. Chem. Eng. **4**, 151 (1987).
[5] D. A. Bruggeman, Ann. Phys. **28**, 160 (1937).
[6] A. Acrivos and E. Chang, Phys. Fluids **29**, 1 (1986); E. Chang, B. S. Yendler, and A. Acrivos, in *Proceedings of the SIAM Workshop on Multiphase Flows*, edited by G. Papanicolaou (SIAM, Philadelphia, 1986), pp. 35–54.
[7] Z. Hashin and S. Shtrikman, J. Appl. Phys. **33**, 3125 (1962).
[8] M. Beran, Nuovo Cimento **38**, 771 (1965).
[9] G. W. Milton, Phys. Rev. Lett. **46**, 542 (1981).
[10] S. Torquato and I. C. Kim, Appl. Phys. Lett **55**, 1847 (1989).
[11] L. Pontryagin, A. Andronow, and A. Witt, Zh. Eksp. Teor. Fiz. **3**, 172 (1933).
[12] S. Lifson and J. L. Jackson, J. Chem. Phys. **36**, 2410 (1962).
[13] J. B. Keller, J. Math. Phys. **5**, 548 (1964); K. S. Mendelson, J. Appl. Phys. **46**, 917 (1975).
[14] W. T. Perrins, D. R. McKenzie, and R. C. McPhedran, Proc. R. Soc. London Ser. A **369**, 207 (1979).
[15] N. Metropolis, A. W. Rosenbluth, M. N. Rosenbluth, A. N. Teller, and E. Teller, J. Chem. Phys. **21**, 1087 (1953).
[16] F. Lado, J. Chem. Phys. **49**, 3092 (1968).
[17] W. W. Wood, J. Chem. Phys. **48**, 415 (1968).
[18] S. B. Lee and S. Torquato, J. Chem. Phys. **89**, 3258 (1988).
[19] G. W. Milton, J. Appl. Phys. **52**, 5294 (1981).
[20] S. Torquato and F. Lado, Proc. R. Soc. Lond. A **417**, 59 (1988).
[21] A. S. Sangani and C. Yao, Phys. Fluids **31**, 2426 (1988).
[22] C. A. Miller and S. Torquato, J. Appl. Phys. (in press).
[23] P. P. Durand and L. H. Ungar, Int. J. Numer. Methods Eng. **26**, 2487 (1988).
[24] P. M. Richards, J. Chem. Phys. **85**, 3520 (1986); P. M. Richards, Phys. Rev. B **35**, 248, (1987).
[25] S. B. Lee, I. C. Kim, C. A. Miller, and S. Torquato, Phys. Rev. B **39**, 11833 (1989).
[26] L. M. Schwartz and J. R. Banavar, Phys. Rev. B **39**, 11965 (1989).
[27] I. C. Kim and S. Torquato, to be published.